ESC European Society of Cardiology

Cardiovascular Research (2018) **114**, 880–893
doi:10.1093/cvr/cvy016

Loss of KCNK3 is a hallmark of RV hypertrophy/dysfunction associated with pulmonary hypertension

Mélanie Lambert[1,2,3†], Angèle Boet[1,2,3,4†], Catherine Rucker-Martin[1,2,3], Pedro Mendes-Ferreira[5], Véronique Capuano[1,2,3], Stéphane Hatem[6], Rui Adão[5], Carmen Brás-Silva[5], Aurélie Hautefort[1,2,3], Jean-Baptiste Michel[7], Peter Dorfmuller[1,2,3], Elie Fadel[1,2,3,8], Tom Kotsimbos[9], Laura Price[10], Philippe Jourdon[1,2,3], David Montani[1,2,3], Marc Humbert[1,2,3], Frédéric Perros[1,2,3], and Fabrice Antigny[1,2,3]*

[1]Univ. Paris-Sud, Faculté de Médecine, Université Paris-Saclay, Le Kremlin Bicêtre 94270, France; [2]Assistance Publique Hôpitaux de Paris, Service de Pneumologie, Hôpital Bicêtre, Le Kremlin Bicêtre 94270, France; [3]Inserm UMR_S 999, Hôpital Marie Lannelongue, Le Plessis Robinson 92350, France; [4]Réanimation des Cardiopathies Congénitales, Univ. Paris-Sud, Hôpital-Marie-Lannelongue, Le Plessis-Robinson, France; [5]Department of Surgery and Physiology, Faculty of Medicine, Cardiovascular Research Centre, University of Porto, 4200-319 Porto, Portugal; [6]Département de Cardiologie, INSERM UMR_S1166, ICAN, Assistance Publique-Hôpitaux de Paris, Hôpital Pitié-Salpêtrière 75013, France; [7]INSERM UMR_S1148, Paris7, Denis Diderot University, Xavier Bichat Hospital, 75018, Paris, France; [8]Service de Chirurgie Thoracique, Centre Chirurgical Marie Lannelongue, Le Plessis-Robinson, France; [9]Department of Respiratory Medicine, Alfred Hospital, Monash University, Melbourne, VIC 3181, Australia; and [10]National Pulmonary Hypertension Service, Royal Brompton Hospital, London SW3 6NP, UK

Received 12 July 2017; revised 22 December 2017; editorial decision 14 January 2018; accepted 18 January 2018; online publish-ahead-of-print 19 January 2018

Time for primary review: 50 days

Aims Mutations in the *KCNK3* gene, which encodes for an outward-rectifier K^+ channel, have been identified in patients suffering from pulmonary arterial hypertension (PAH), and constitute the first described channelopathy in PAH. In human PAH and experimental pulmonary hypertension (PH), we demonstrated that KCNK3 expression and function are severely reduced in pulmonary vascular cells, promoting PH-like phenotype at the morphologic and haemodynamic levels. Since KCNK3 channel is also expressed in both the human and rodent heart, we aimed to elucidate the pathophysiological role of KCNK3 channel in right ventricular (RV) hypertrophy (RVH) related to PH.

Methods and results Using whole-cell Patch-clamp technique, we demonstrated that KCNK3 is predominantly expressed in adult rat RV cardiomyocytes compared to the left ventricle cardiomyocytes and participates in the repolarizing phase of the RV action potential. We revealed a reduction in KCNK3 function prior to development of RVH and the rise of pulmonary vascular resistance. KCNK3 function is severely reduced in RV cardiomyocytes during the development of RVH in several rat models of PH (exposure to monocrotaline, chronic hypoxia, and Sugen/hypoxia) and chronic RV pressure overload (pulmonary artery banding). In experimental PH, we revealed a reduction in KCNK3 function before any rise in pulmonary vascular resistance and the development of RVH. KCNK3 mRNA level is also reduced in human RV tissues from PAH patients compared to non-PAH patients. In line with these findings, chronic inhibition of KCNK3 in rats with the specific inhibitor (A293) induces RV hypertrophy which is associated with the re-expression of foetal genes, RV fibrosis, RV inflammation, and subsequent loss of RV performance as assessed by echocardiography.

Conclusion Our data indicate that loss of KCNK3 function and expression is a hallmark of the RV hypertrophy/dysfunction associated with PH.

Keywords K2P3.1 • RV dysfunction • MCT • TASK-1 • Ito • A293 • KCNK3 inhibitor

* Corresponding author. Tel: +33 1 40 94 22 99; fax: +33 1 40 94 25 22, E-mail: fabrice.antigny@u-psud.fr

† The first two authors contributed equally to the study.

1. Introduction

Pulmonary hypertension (PH) is a severe and lethal cardiopulmonary disease clinically characterized by an increase in the mean pulmonary arterial pressure ≥ 25 mmHg at rest.[1] PH is the consequence of an increase in pulmonary vascular resistance due to remodelling of the small distal pulmonary arteries and arterioles (diameter <500 μm), causing adaptive right ventricular (RV) hypertrophy and when unchecked, right heart failure.[2] Cardiac hypertrophy is the primary mechanism preserving myocardial pump function in the setting of cardiac stress due to pressure overload induced by hypertension. Unlike left ventricular hypertrophy, RV hypertrophy related to PH is relatively weakly characterized at the electrophysiological level. Over last two decades, several predisposing genes have been identified in pulmonary arterial hypertension (PAH), mainly in the transforming growth factor β superfamily signalling pathway.[3] In 2013, six loss of function mutations in *KCNK3* gene were identified in familial PAH and sporadic PAH.[4] More recently, Navas *et al.* identified two additional mutations in the *KCNK3* gene in PAH patients, and described the first PAH patient with an homozygous *KCNK3* mutation associated with an aggressive form of PAH.[5] The KCNK3 protein is an outward-K^+ channel characterized by the presence of four transmembrane domains and two pore domains per sub-unit,[6] (K2P), also called TASK1 (Twik-related-acid-sensitive-K^+ channel) or K2P3.1. The KCNK3 channel exhibits several particularities including minimal voltage sensitivity, extracellular pH sensitivity, inhibition by α1A-adrenergic receptor stimulation, resistance to the classical K^+ channels inhibitors, and insensitivity to cytoplasmic Ca^{2+}.[7,8] KCNK3 channels are expressed in the heart of multiple species including zebrafish, chicken, mice, rats, dogs, and humans.[9] In human and rodents, KCNK3 is known to be expressed in both atria and ventricles.[10,11] Genetic ablation or pharmacological inhibition of KCNK3 channels results in prolongation of cardiac LV action potential and QT interval in mice.[8,12,13] In human, an over-activation of KCNK3 is associated with right atrial fibrillation, suggesting the potential of KCNK3 inhibition as a novel therapeutic option for atrial fibrillation therapy.[11] However, the role played by defective KCNK3 channel in RV dysfunction occurring in PH is still unknown.

We recently demonstrated that pulmonary KCNK3 expression and function were severely reduced in idiopathic and heritable PAH (associated to *BMPR2* mutations), and in pulmonary vascular cells isolated from a rat model of severe experimental pulmonary hypertension [monocrotaline (MCT)-rats].[14] Interestingly, it has been previously reported that transient outward-K^+ current (I_{to}) is reduced in the RV 4 weeks after MCT exposure and that this associated with decreased mRNA expression of several voltage-gated K^+ channels (Kv).[15]

In the present study, we investigated by a combination of echocardiography, molecular biology, and patch-clamp approaches, the expression, and the function of KCNK3 in the RV and LV during the development of RV hypertrophy secondary to severe PH. As well as using several experimental rat models [PH induced by MCT exposure, by chronic hypoxia and by Sugen/hypoxia exposure and in chronic RV pressure overload (induced by pulmonary artery banding) (PAB)]. RV tissues from both PAH and non-PAH patients were also examined. Finally, we explored analysed the consequences of chronic *in vivo* inhibition of KCNK3 in rats with a selective KCNK3 channel blocker (A293).

2. Methods

An expanded methods section is provided in the Supplementary material online.

2.1 Materials

Tetraethylammonium, 4-AminoPyridin (4-AP), MCT, collagenase A was obtained from Sigma. The selective blocker of KCNK3, A293 (KCNK3 inhibitor) (2-(butane-1-sulfonyl-amino)-N-[1-(R)-(6-methoxypyridin-3-yl)-propyl]-benz-amide), was kindly provided by Sanofi-Aventis (R&D). The IC50 value for blockade of KCNK3 channels by A293 was estimated at 245.2 ± 113.5 nM.[8,16] In addition, in Xenopus oocyte expression system, A293/KCNK3 inhibitor at 200 nM or 1 μM was demonstrated to have no significant impact on human K^+ channels function including Kv1.5, Kv4.3, hERG (Kv11.1), KCNQ1 (Kv7.1)/KCNE1, Kir2.1, Kir2.2, and Kir2.3 channels.[8,16]

2.2 Patients

Non-PAH human cardiac tissues (right and left ventricle) were obtained at the time of heart transplantation from five patients with left ventricular dysfunction (2 females and 3 males with mean age 52 years). PAH human cardiac tissues (right and left ventricle) were obtained at the time of heart-lung transplantation from four PAH patients: (*Table 1*). PAH patients studied were part of the French Network on PH, a program approved by our institutional Ethics Committee and who had given their written informed consent (Protocol N8CO-08- 003, ID RCB: 2008-A00485-50, approved 18 June 2008). All human tissue was obtained with written and informed consent from transplant recipients or families of organ donors in accordance to the declaration of Helsinki.

2.3 Animals

The animal facility is licensed by the French Ministry of Agriculture (agreement N° B92-019-01). This study was approved by the Committee on the Ethics of Animal Experiments CEEA26 CAP Sud. Animal experiments were approved by the French Ministry of Agriculture for animal experiments N° A92–392. The animal experiments were performed conforming with the guidelines from Directive 2010/63/EU 22 September 2010 of the European Parliament on the protection of animals used for scientific purposes and complied with French institution's guidelines for animal care and handling.

2.4 Statistical analysis

All values are expressed as the mean ± SEM. Data were analysed with use of the Student *t*-test or one-way analysis of variance and Dunnett's multiple comparisons test were performed with GraphPad Prism software (GraphPad, version 6.0 for Windows). For patch-clamp experiments, we used a nested anova to a mixed effects model. Here, control vs. different treatment was treated as a fixed effect, while Rat was treated as a random effect. Nested anova were performed using R software (version 3.0.1 statistical) (R Foundation, www.r-project.org).[17] Differences were considered statistically significant at $P < 0.05$ *, $P < 0.01$ **, $P < 0.001$***.

3. Results

3.1 KCNK3 channels are functionally expressed in adult rat RV cardiomyocytes and contribute to action potential repolarization

Using whole-cell patch-clamp experiments, KCNK3 current (I_{KCNK3}) was recorded in isolated RV cardiomyocytes. To specifically isolate I_{KCNK3} from outward-K^+ currents, we applied the KCNK3 inhibitor

Table 1 Clinical characteristic for patients with PAH used for QPCR experiments

Age at diagnosis (years)	Gender	NYHA class	6MWD (m)	mPAP (mmHg)	PVR (dyn*s/cm^{-5})	WHO classification	Mutations in *BMPR2, KCNK3, EIF2AK4 genes*	PAH therapy
14	F	4	375	93	1520	1	no	Prostacyclin PDE5i ERA
34	M	4	250	44	681	1	no	Prostacyclin PDE5i ERA
49	M	4	MD	53	MD	1	no	Prostacyclin PDE5i ERA
54	M	4	MD	64	MD	Eisenmenger syndrome	no	MD

6MWD, 6-min walk distance; mPAP, mean Pulmonary Arterial Pressure; PVR, Pulmonary vascular resistance.

Table 2 List of the gene expression assays (Life Technology) used in this study

Gene	Primer reference	Species
KCNK3	Rn04223042_m1	Rat
KCNK9	Rn00755967_m1	Rat
GAPDH	Rn01775763_g1	Rat
Kv4.3	Rn04339183_m1	Rat
Kv4.2	Rn00581941_m1	Rat
Kv1.5	Rn00564245_s1	Rat
Kv2.1	Rn00755102_m1	Rat
Kir2.1	Rn02533449_s1	Rat
TNF-α	Rn01525859_g1	Rat
IL-6	Rn01489669_m1	Rat
GP-130	Rn01410330_m1	Rat
TGIF2	Rn01536049_g1	Rat
Ccl2	Rn00580555_m1	Rat
IL-17Ra	Rn01757168_m1	Rat
CCL1	Rn01752376_m1	Rat
CXCL1	Rn00578225_m1	Rat
MYH6	Rn00691721_g1	Rat
MYH7	Rn01488777_g1	Rat
Col1a1	Rn01463848_m1	Rat
Col3a1	Rn01437681_m1	Rat
BNP	Rn00580641_m1	Rat
ANP	Rn00664637_g1	Rat
KCNK3	Hs00605529_m1	Human
18S	Hs03003631_g1	Human

compound at 200 nmol/L, that specifically inhibits KCNK3 channels at this concentration.[8,14] K^+ currents were recorded in RV cardiomyocytes under control conditions and 3 min after applying KCNK3 inhibitor (*Figure 1A* and *B*) and then the I_{KCNK3} was measured at the end of depolarizing pulse (*Figure 1C*). In control RV myocytes, KCNK3 inhibitor reduced K^+ current by 10–15% at +80 mV (*Figure 1B–C*). As expected, immunofluorescence labelling revealed that KCNK3 channels were mainly expressed at sarcolemmal level in control RV cardiomyocytes (*Figure 1D*). In order to determine the contribution of I_{KCNK3} to the repolarizing phase of RV action potential, we measured the effect of the KCNK3 inhibitor on action potential duration (APD). As shown in *Figure 1E*, the KCNK3 inhibitor led to a prolongation of APD with slightly but significant depolarized resting membrane potential (*Figure 1E*, right panel). In control RV cardiomyocytes, APD at 0 mV was not affected by pharmacological inhibition of KCNK3 channels (*Figure 1F*) whereas, APD at –30 mV and APD at –60 mV were significantly increased.

3.2 RV hypertrophy and dysfunction appears 2 weeks after MCT-exposure

To assess the time course of RV dysfunction in MCT-exposed rats, echocardiographic analyses were performed during the development of PH (1, 2, and 3 weeks after MCT-exposure, W1, W2, and W3, respectively). Different shapes and flow pattern of RV outflow were observed and illustrated in *Figure 2A* (mid systolic notch, micro flow, and saber). Pulmonary artery acceleration time (PAAT) was the earliest parameter to change, and was significantly shortened from W2, demonstrating a higher resistive profile in PA tract with acceleration of RV ejection (*Figure 2B*). Velocity-time integral (VTI) was significantly decreased at W2 and W3, reflecting the establishment of pulmonary flow reduction (*Figure 2C*). We also observed at W3 an increase in RV end diastolic diameter (RVEDD) (*Figure 2D*) and RV wall thickness (*Figure 2E*). At W3, we measured significant impairment of RV fractional shortening (FS) (*Figure 2F*), without any significant modification of cardiac index (CI) in MCT-rats (*Figure 2G*). We also observed at W3 interventricular septum curve deviation of type 2 (flat) or type 3 (right to left deviation) (see Supplementary material online, *Figure S1*). We also measured a significant decrease in Tricuspid annular plane systolic excursion (TAPSE, not shown). However, tissue doppler derived tricuspid annulus systolic velocity (s') and RV ejection time (RVET) were unmodified. These data demonstrated a progressive RV hypertrophy and dysfunction in MCT- rats, which begins from 2 weeks, with rapid deterioration of RV function from W3.

3.3 Progressive increase in APD during the development of RV hypertrophy in MCT-rats

In accordance with echocardiography analyses, we observed a progressive and significant increase in mean pulmonary arterial pressure in

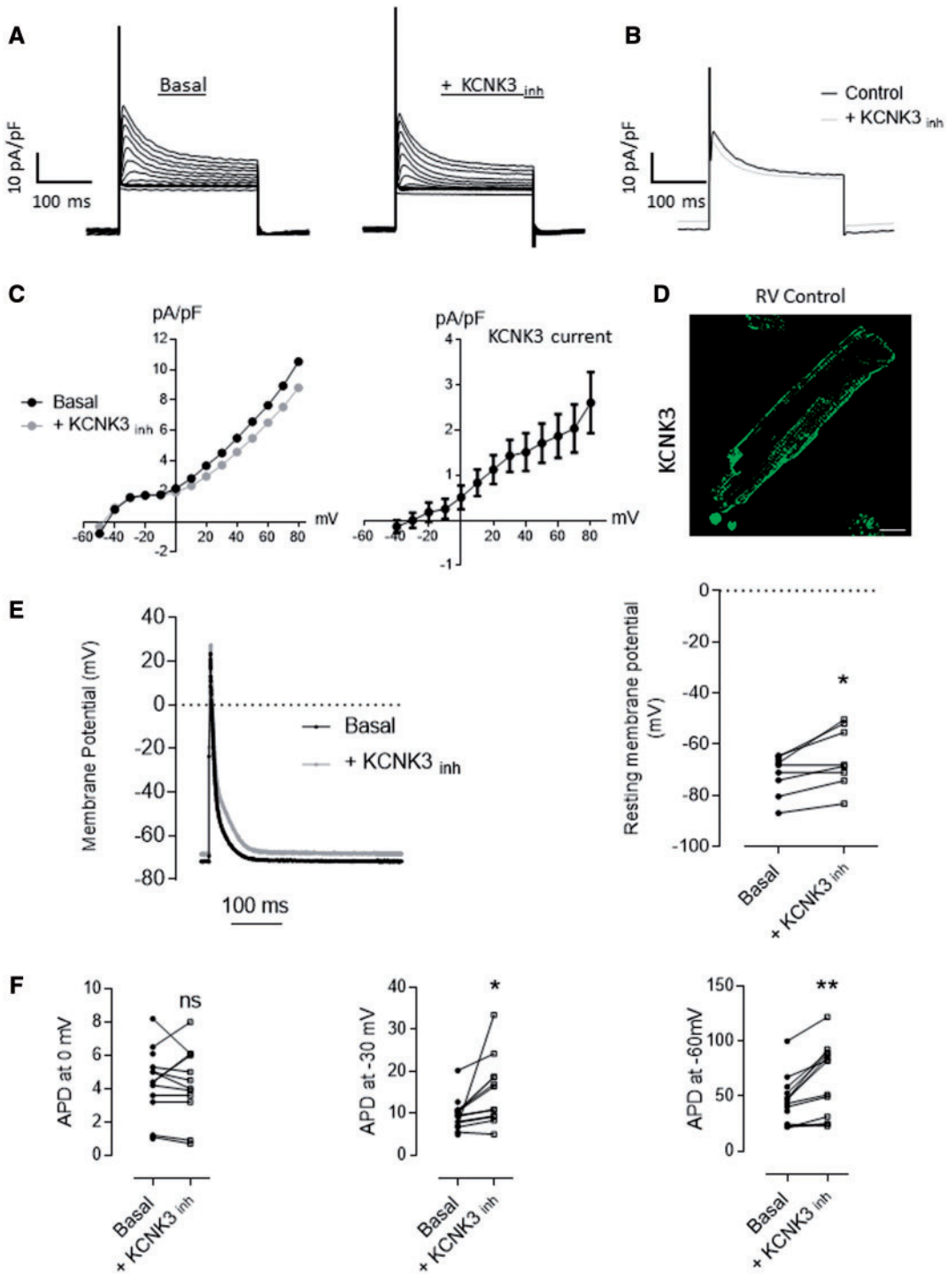

Figure 1 KCNK3 channels function in rat RV cardiomyocytes. (***A*** and ***B***) Representative outward-K^+ current traces recorded on isolated RV cardiomyocytes from control rats, in basal condition (left panel), in the presence of 200 nmol/L A293 (KCNK3 inhibitor, $KCNK3_{inh}$) (right panel). (***C***) Left panel, K^+-current-voltage relationship in RV cardiomyocytes in basal (black trace) and in the presence of the $KCNK3_{inh}$ (grey trace). Right panel, typical KCNK3 current-voltage relationship. (***D***) Immunolabelling and confocal imaging of KCNK3 in isolated RV cardiomyocytes from control rats. KCNK3 expression is shown in green. Scale bar = 10 µm. (***E***) Left panel: Representative AP in RV cardiomyocytes from control rat in the absence (black trace) and after perfusion of the $KCNK3_{inh}$ (grey trace). Right panel: Average resting membrane potential before and after the $KCNK3_{inh}$ application. (***F***) Analysis of action potential duration (APD) at 0 mV, at –30 mV and at –60 mV of membrane repolarization in basal conditions and in presence of 200 nmol/L the $KCNK3_{inh}$ (12–14 cells from four different rats). Compared with control $P < 0.05$*, $P < 0.01$** (Nested anova for patch-clamp experiments).

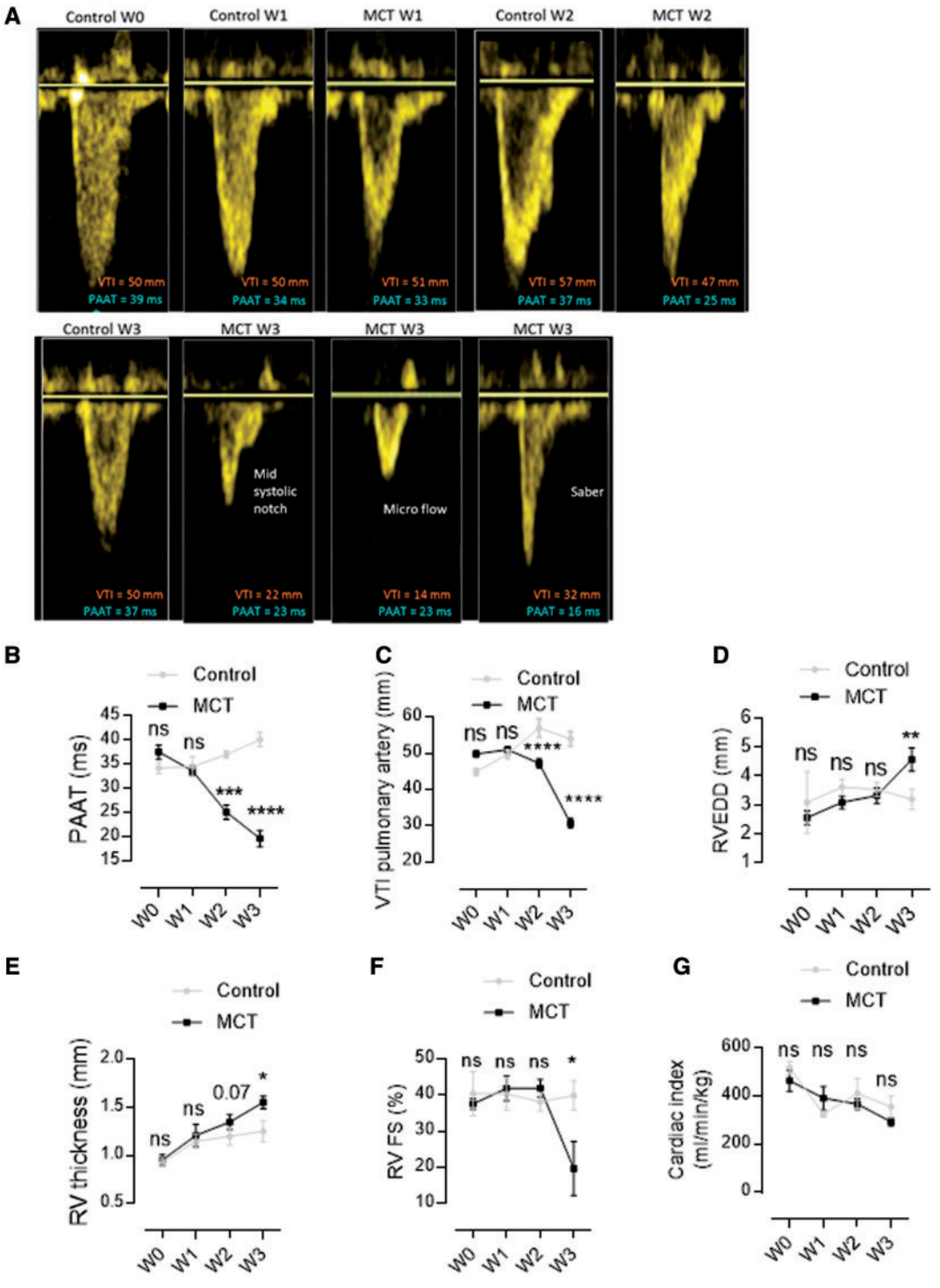

Figure 2 Characterization of RV dysfunction at echocardiographic level in MCT-PH rats. (***A***) Representative pulmonary artery flow through the pulmonary valve in controls and MCT rats at 1 week, 2 and 3 weeks following MCT-exposure. (***B***) Quantification of the pulmonary acceleration time (PAAT). (***C***) Velocity Time Integral (VTI). (***D***) Right ventricular ejection time (RVET). (***E***) RV thickness (mm). (***F***) right ventricle fractional shortening (RV FS). (F) Cardiac index (CI) (mL/min/kg). **(**7–12 different rats). Compared with control $P < 0.05$*, $P < 0.01$**, $P < 0.001$*** (One-way anova followed by Dunnett's).

MCT-exposed rats (W2 and W3) (*Figure 3A*, Left panel). We also measured a progressive RV hypertrophy through the Fulton index (W2 and W3) (*Figure 3A*, Right panel). Cardiac hypertrophy is well described to be associated with re-expression of foetal genes. At W3, we observed the switching of myosin heavy chain isoforms from α (adult-MYH6) to β (foetal-MYH7) (*Figure 3B–C*) (Table 2). We also found a rise in the expression of biochemical markers of ventricular dysfunction such as atrial natriuretic peptide (ANP, encoding by *NPPA* gene) and B-type

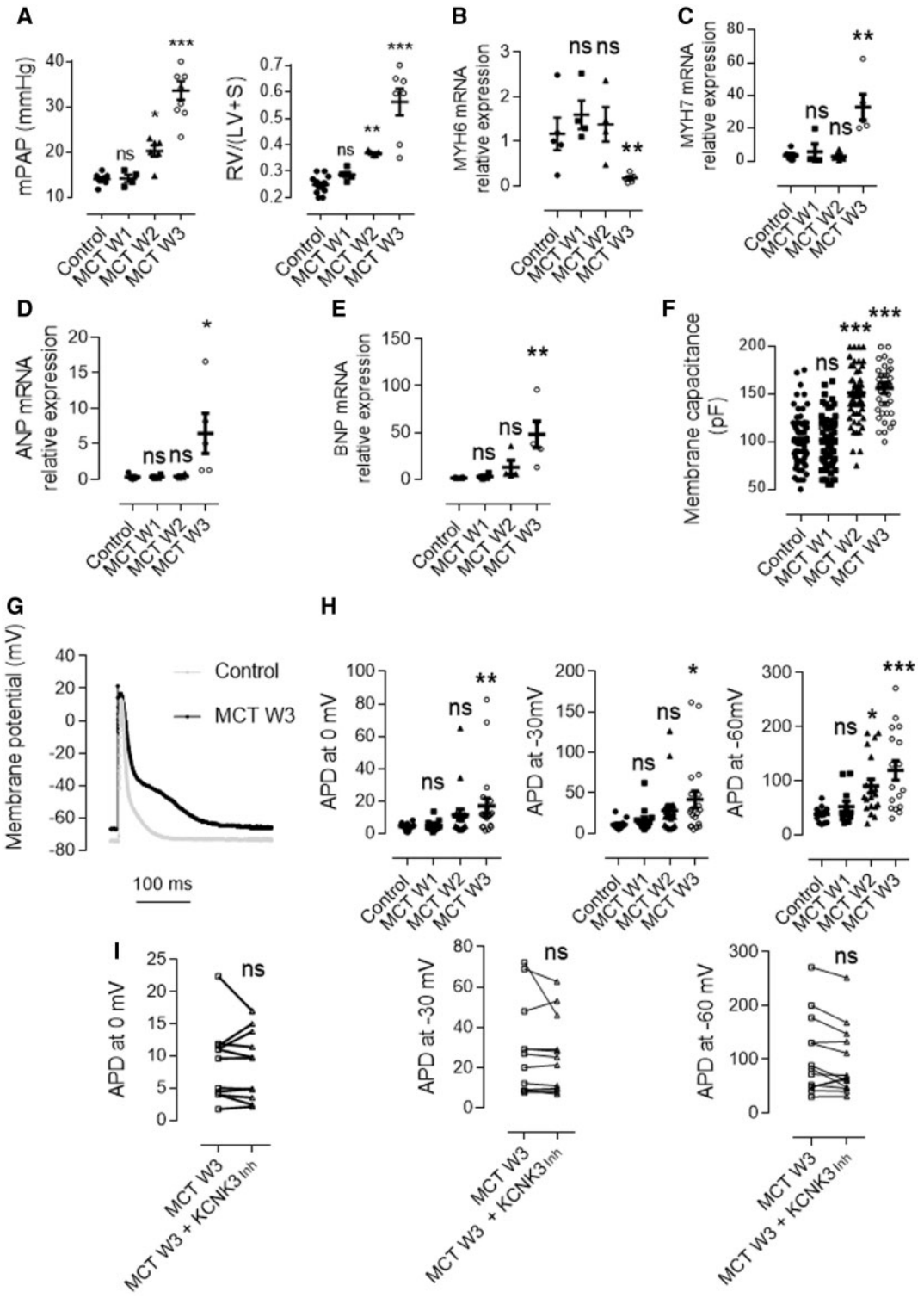

Figure 3 Characterization of the RV hypertrophy at cellular and molecular level in MCT-rats. (***A***) Mean pulmonary arterial Pressure (mPAP) in control and MCT-PH rats. Right panel, Fulton's index [weight ratio of RV and (LV + septum)] (n = 5–10 rats). (***B–E***) mRNA expression of MYH6 (B), MYH7 (C), ANP (D), and BNP (E) in RV from control and MCT rats (at W1, W2, and W3) (n = 5 rats). (***F***) RV cardiomyocytes cell capacitance from control and MCT rats (70–46 cells from five different rats). (***G***) Representative membrane potential of RV cardiomyocytes from control rats and 3 weeks after MCT-exposure. Grey trace: control condition. Black trace: MCT W3. (***H***) Analysis of RV action potential duration (APD) at 0 mV, APD at –30 mV, and APD at –60 mV of membrane repolarization in control rats and MCT rats (n = 20 cells from four different rats). (***I***) Analysis of RV APD at 0 mV, at –30 mV, and at –60 mV of membrane repolarization in MCT W3 cardiomyocytes with or without KCNK3 inhibitor (n = 10 cells from three different rats). Compared with control; ns = non-significant, $P < 0.05$*, $P < 0.01$**, $P < 0.001$*** (Nested anova for patch-clamp experiments. Other experiments were analysed using one-way anova followed by Dunnett's).

natriuretic peptide (BNP, encoding by *NPPB* gene) (*Figure 3D–E*). The hypertrophy of RV cardiomyocytes was confirmed at W2 and W3 using measures of the cell membrane capacitance (*Figure 3F*).

In accordance with RV dysfunction previously observed at W2 and W3, we found a significant prolongation of APD (*Figure 3G–H*). Interestingly, while KCNK3 channels inhibition (by KCNK3 inhibitor at 200 nmol/L) increased APD in control RV cardiomyocytes (*Figure 1E–F*), it had no effect on APD in isolated RV cardiomyocytes from 3 weeks MCT-rats (*Figure 3I*), suggesting that KCNK3 channels were no longer functional at this time.

3.4 Reduction of I_{KCNK3} precedes the establishment of RV hypertrophy and RV dysfunction in MCT-rats

While the KCNK3 inhibitor significantly reduced K^+ currents in control RV cardiomyocytes (*Figure 1C*), it had no impact on K^+ currents 3 weeks after MCT exposure (*Figure 4A*), indicating that I_{KCNK3} was strongly reduced in hypertrophied RV cardiomyocytes. Indeed, I_{KCNK3} was reduced by three-fold in PH (W1, W2, and W3) compared to control condition (*Figure 4B–C*), indicating that I_{KCNK3} reduction precedes RV dysfunction. Moreover, at W1, immunofluorescence labelling revealed a loss of sarcolemmal localization of KCNK3 and a loss of fluorescence intensity on the cardiomyocyte surface more pronounced at W3, suggesting an early reduction of KCNK3 expression (*Figure 4D*). According to these results, KCNK3 mRNA levels were strongly reduced in RV from PH rats (*Figure 4E*), while KCNK9 which is known to functionally dimerize with KCNK3[18,19] was undetectable in rat cardiac tissue (*Figure 4F*). We performed quantitative RT-PCR to quantify KCNK3 mRNA expression in human RV tissue from five non-PAH patients and four PAH patients. Having established baseline KCNK3 expression, at mRNA level, in non-PAH ventricular tissues (*Figure 4G*) we demonstrated that KCNK3 expression was strongly reduced in RV tissues from PAH patients (*Figure 4H*) (Table 2). Interestingly, in rat model, patch-clamp recordings, and quantitative-PCR showed that KCNK3 was predominantly expressed in RV cardiomyocytes compared to LV (see Supplementary material online, *Figure S2A–B*). In contrast to RV from MCT-rats, KCNK3 function, expression, and localization were unchanged in LV following MCT treatment (see Supplementary material online, *Figure S2C–D*), and the cell membrane capacitance of LV cardiomyocytes was unchanged during the development of PH (see Supplementary material online, *Figure S2E*). Similarly to I_{KCNK3}, I_{to} was significantly higher in RV cardiomyocytes compared to LV (see Supplementary material online, *Figure S2F*) in accordance with the higher expression of Kv4.2 and Kv4.3 in RV compared to LV (see Supplementary material online, *Figure S2G*). I_{to} was not affected in LV after MCT-exposure (see Supplementary material online, *Figure S2H*) associated with the unaffected expression of Kv4.2 and Kv4.3 (see Supplementary material online, *Figure S2I*). In line with the steadiness of I_{KCNK3} in LV from MCT, I_{sus} were also unmodified in MCT-rats (data not shown). Finally, no modification of I_{K1} was recorded (see Supplementary material online, *Figure S3*). These results demonstrated the specific K^+ current alteration of in the RV side compared to the LV side in MCT rats.

We next recorded I_{KCNK3} in RV cardiomyocytes from two additional PH rats model: the chronic hypoxia- rats and the Sugen/hypoxia-induced PH. As expected, both models are associated with marked RV hypertrophy response secondary to the development of PH (see Supplementary material online, *Figure S4A–D*). We also demonstrated that the KCNK3 current is severely reduced in RV cardiomyocytes isolated from PH rats exposed to Sugen/hypoxia and chronic hypoxia (*Figure 4I* and *J*, respectively). Cell capacitance measurement (reflecting cell size) confirmed the RV hypertrophy at the cellular level (see Supplementary material online, *Figure S4A–E*). Finally, we analysed by Quantitative RT-PCR the KCNK3 mRNA expression in the RV of rats with RV pressure overload induced by PAB as compared to Sham rats. We demonstrated that KCNK3 expression was strongly reduced in RV tissues from PAB rats (*Figure 4K*), while KCNK3 expression was unchanged in the LV compartment (see Supplementary material online, *Figure S4F*).

3.5 Similarly to I_{KCNK3}, I_{to}, and I_{sus} are reduced during the establishment of RV hypertrophy

We demonstrated that I_{KCNK3} contributes to the action potential repolarization of RV cardiomyocytes, however, transient (I_{to}) and sustained (I_{sus}) outward-K^+ current are also crucially important for action potential repolarization. Thus, we analysed I_{to} and I_{sus} during the establishment of RV hypertrophy. These recordings indicated that I_{to} was progressively reduced (*Figure 5A–C*) in association with a strong decrease in I_{to} channels Kv4.2 and Kv4.3 mRNA expression (*Figure 5D*). Moreover, I_{to} was reduced without modification of inactivation time constants (data not shown). We also demonstrated that I_{sus} (steady-state-K^+ current) was reduced at W1, W2, and W3 (*Figure 5E*) associated with a reduced expression of Kv1.5, Kv2.1 in RV hypertrophy (see Supplementary material online, *Figure S6A–B*). This decrease in I_{sus} could partly be attributed to KCNK3 loss of function (*Figure 4*) since I_{KCNK3} was measured at the steady-state-K^+ current.

Finally, we observed a decrease of the background inward-rectifier current (I_{K1}) in RV MCT-rats (see Supplementary material online, *Figure S4A–B*) with a significant reduction of Kir2.1 mRNA (coding for I_{K1} channel) at W3 (see Supplementary material online, *Figure S4C*). All these alterations (I_{KCNK3}, I_{to}, I_{K1}) contribute together to abnormal AP repolarization in RVH.

3.6 Chronic inhibition of KCNK3 induced molecular and electrophysiological alterations related to RV hypertrophy

We demonstrated that chronic *in vivo* inhibition of KCNK3 with KCNK3 inhibitor compound (A293 at 10 mg/kg/day) (KCNK3 inhibited-rats) abolished I_{KCNK3} in RV cardiomyocytes 1 week (W1) and 4 weeks (W4) after KCNK3 inhibitor-exposure (see Supplementary material online, *Figure S5A*), while KCNK3 mRNA levels were unchanged (see Supplementary material online, *Figure S5B*). At these time point, I_{to} and I_{sus} were also reduced by 30% and by 35%, respectively (see Supplementary material online, *Figure S5C–D*) in RV cardiomyocytes without any change in the expression of the corresponding channels (see Supplementary material online, *Figure S7A–B*). No modification of the I_{to} inactivation time constants was observed (data not shown), eliminating a non-specific effect of KCNK3 inhibitor on current properties and I_{K1} was unchanged in KCNK3 inhibited-rats (data not shown). In LV cardiomyocytes from KCNK3-inhibited rats, I_{to}, I_{sus}, and I_{K1} were unchanged compared to control condition (see Supplementary material online, *Figure S7C–F*).

We measured a significant increase in cell membrane capacitance at W4, demonstrating RV cardiomyocyte hypertrophy (see Supplementary material online, *Figure S5E*). MYH6 mRNA was decreased at W1 and W4 whereas MYH7 mRNA increased only at W4. In addition, we showed a trend for increased ANP mRNA at W1 and W4 (see

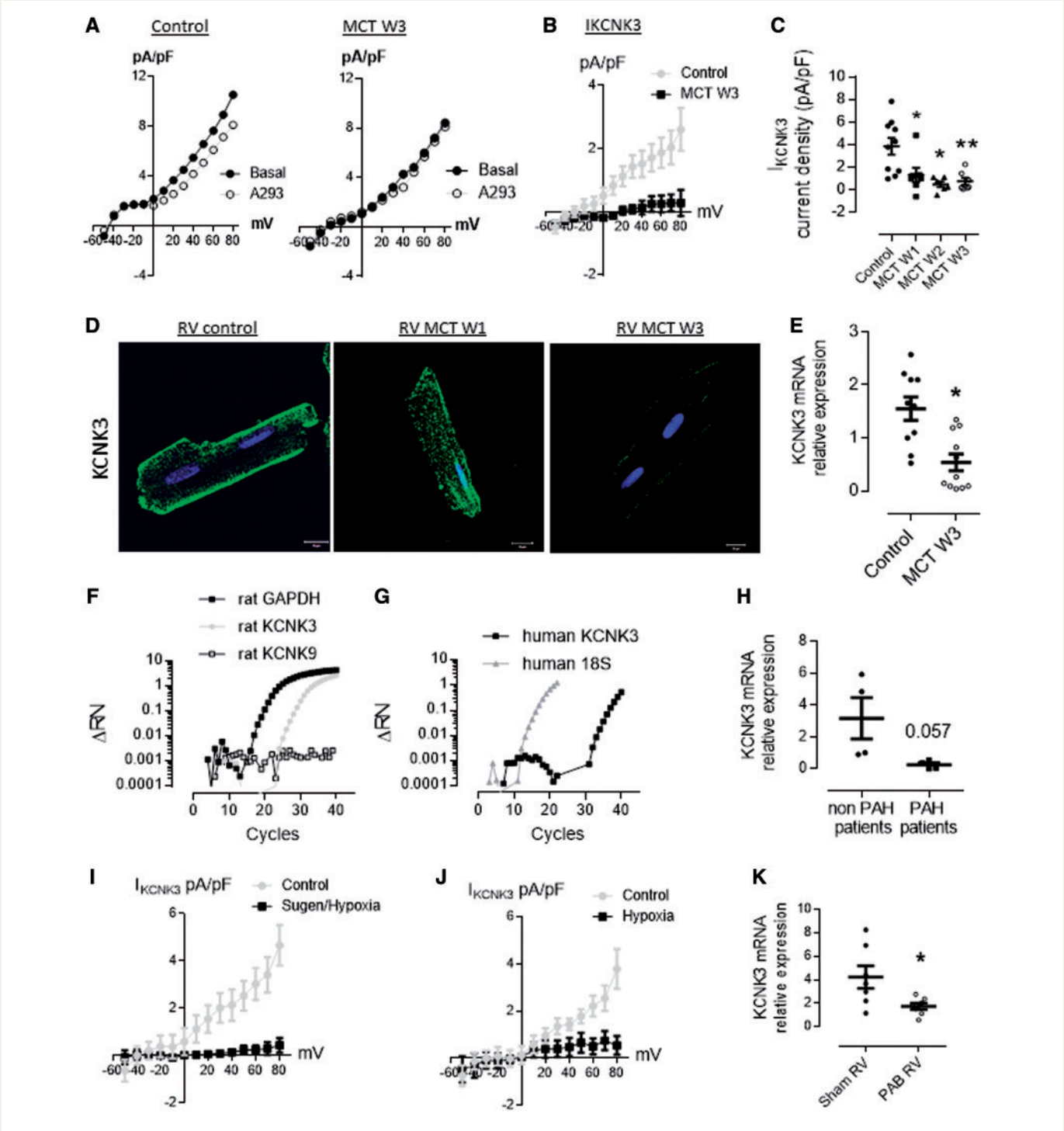

Figure 4 I_{KCNK3} is decreased during the development of RV hypertrophy. (***A***) Current-voltage relationship of K^+ currents in basal (black trace) and in the presence of KCNK3 inhibitor (grey trace) in control and MCT-rats (W3). (***B***) Current-voltage relationship of I_{KCNK3} in RV cardiomyocytes isolated from control and MCT rats (W3). (***C***) Current density (+80 mV) in control (n = 7 cells) and MCT rats (W1, W2, and W3) (10 cells each from three different rats). (***D***) Immunolabelling and confocal imaging of KCNK3 channels in isolated RV cardiomyocytes from control rats and 1 and 3 weeks after MCT exposure. KCNK3 is shown in green and nuclei in blue (DAPI). Scale bar = 10 μm. (***E***) KCNK3 mRNA expression in isolated RV from control and MCT-PH rats (W3) (n = 10 rats). (***F***) Representative amplification of rat KCNK3 mRNA, rat KCNK9 mRNA, and rat GAPDH from RV tissue (n = 5 different rats in control rats). (***G***) Representative amplification of human KCNK3 mRNA and human 18S mRNA in human non-PAH RV tissue. (***H***) KCNK3 mRNA expression in RV tissues from non-PAH patients and PAH patients (n = 4), normalized by 18S mRNA expression. (***I***) Current-voltage relationship of an I_{KCNK3} in RV cardiomyocytes isolated from control and Sugen/hypoxia rats (10 cells from 3–5 different rats). (***J***) Current-voltage relationship of an I_{KCNK3} in RV cardiomyocytes isolated from control and hypoxia rats (10–8 cells from 3–5 different rats). (***K***) KCNK3 mRNA expression in RV tissues from Sham rats and rats subjects to pulmonary artery banding (PAB) (n = 7 different rats). Compared with control. ns = non-significant, $P < 0.05$*, $P < 0.01$** (Nested anova for patch-clamp experiments. Other experiments were analysed using one-way anova followed by Dunnett's).

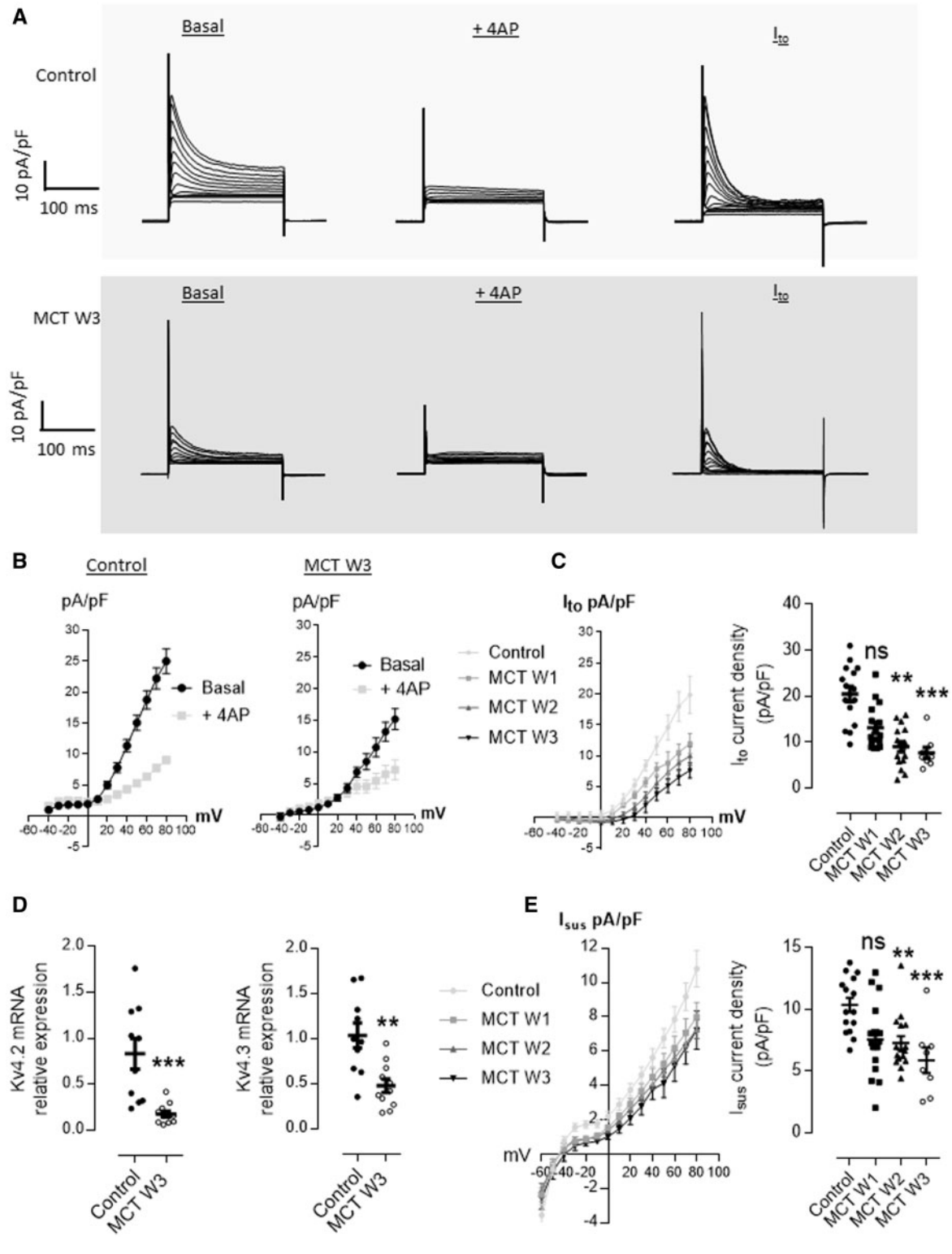

Figure 5 I_{to} and I_{sus} decrease progressively during the development of RV hypertrophy. (***A***) Representative outward-K^+ currents traces recorded on freshly isolated RV cardiomyocytes from control (upper trace) and MCT-rats (W3) (lower trace), in basal conditions (left panel), in the presence of 5 mM 4-AP (middle panel), and the 4-AP sensitive current (Right panel). (***B***) Current-voltage relationship of outward-K^+ currents in basal (black trace) and in presence of 4-AP (grey trace) from control and MCT rats (W3). (***C***) Left panel, Current-voltage relationship of 4-AP-sensitive-K^+ current also called I_{to} in control and MCT-rats (W1, W2, and W3). Right panel, I_{to} current density at +80 mV in each condition (10–8 cells from 3–5 different rats). (***D***) mRNA expression of Kv4.2 (left panel) and Kv4.3 (right panel), in RV isolated from control and MCT-rats (W3) (n = 6–10 rats). (***E***) Left panel, Current-voltage relationship corresponding to I_{sus} in RV cardiomyocytes isolated from control and MCT rats (W1, W2, and W3). Right panel, RV I_{sus} density from control and MCT rats (W1, W2, and W3) (14–8 cells from 3–5 different rats). Compared with control. ns = non-significant, $P < 0.05$*, $P < 0.01$**, $P < 0.001$*** (Nested anova for patch-clamp experiments. Other experiments were analysed using one-way anova followed by Dunnett's).

Supplementary material online, *Figure S5F*). To confirm RV cardiomyocyte hypertrophy we performed staining with FITC-conjugated wheat germ agglutinin (WGA), a member of the lectin family that binds to N-acetyl-D-glucosamine and sialic acid residues found on the surface of cell membranes. We measured a significant increase in the diameter of RV cardiomyocytes in KCNK3 inhibited-rats as compared to vehicle treated rats (*Figure 6I*), while the size of LV cardiomyocytes was unchanged (see Supplementary material online, *Figure S5G*).

3.7 Chronic inhibition of KCNK3 leads to loss of RV performance

Finally, we assessed the consequences of *in vivo* chronic KCNK3 inhibition on cardiac ventricular function by echocardiography examination 4 weeks after KCNK3 inhibitor-exposure. In KCNK3 inhibited-rats PAAT, VTI, and RVET were significantly reduced compared to control (*Figure 6A–B*). Moreover, the RVEDD was reduced (see Supplementary material online, *Figure S8A*). At W1, KCNK3 inhibited-rats showed no significant change in RV function (*Figure 6C*), while RV thickness was increased (see Supplementary material online, *Figure S8B*). Importantly, 4 weeks after KCNK3 inhibitor-exposure, we measured a halving in RV performance (decrease of RV FS) associated with an increase in RV thickness (*Figure 6C* and see Supplementary material online, *Figure S8B*), whereas RV stroke volume was reduced at 4 weeks after KCNK3 inhibitor-exposure (W4) (*Figure 6E*). At W4, LV thickness (see Supplementary material online, *Figure S8C*) and LV FS (*Figure 6D*) were unchanged. In contrary to MCT-rats where LV end diastolic diameter (LVEDD) was decreased (data not shown), LVEDD was significantly increased in KCNK3 inhibited-rats (at W4) (see Supplementary material online, *Figure S8D*). We also observed an increase in heart rate in KCNK3 inhibited-rats (*Figure 6F*). That was inversely proportional to a significant decrease in RV stroke volume thereby giving RV cardiac output measures that were unchanged in KCNK3 inhibited-rats (*Figure 6G*). No variation in TAPSE was observed in KCNK3 inhibited-rats (data not shown). These results highlight the severe abnormalities of RV function induced by KCNK3 inhibition.

3.8 Chronic inhibition of KCNK3 leads to abnormal action potential prolongation and RV fibrosis

As shown in *Figure 7A*, action potentials were significantly prolonged in RV cardiomyocytes from KCNK3 inhibited-rats at 0 mV, –30 mV, and –60 mV (*Figure 7A–B*). We also recorded a significant depolarization of resting membrane potential (*Figure 7C*). In KCNK3 inhibited-rats, we also observed early-after depolarization events in some RV cardiomyocytes (data not shown). Moreover, using Sirius red staining we showed a significant increase in RV fibrosis in KCNK3 inhibited-rats as compared to control rats (*Figure 7D–E*) associated with an increase in mRNA level of Col1A1, while Col3A1 mRNA was unchanged (*Figure 7F*).

Finally, quantitative-PCR experiments demonstrated significantly higher mRNA expression of interleukin 6 (IL-6) in the RV from KCNK3 inhibited-rats while mRNA expression of gp130 (IL-6 receptor subunit) was not significantly increased in these rats. We also measured a significant increase in TGIF2 (TGFB-Induced Factor 2) in RV from KCNK3-inhibited rats (*Figure 7G*), while mRNA expression of TNFα, IL-17Ra, CXCL12, CXCL1, CCl2 were not significantly modified in RV tissues from KCNK3-inhibited- rats (see Supplementary material online, *Figure S9*) (Table 2). Additionally, we showed a significant increase in the number of Toluidine Blue (mature mast cells markers) positive cells in RV tissues from KCNK3-inhibited-rats, suggesting a RV accumulation/recruitment of mature mast cells in KCNK3-inhibited-rats (*Figure 7H*). Other inflammatory cells (macrophages and T lymphocytes, respectively, tested by immunostaining against CD68 and CD3) were not present in RV tissues from KCNK3-inhibited rats (data not shown).

4. Discussion

This study has five major findings that taken together underscore the critical importance of altered KCNK3 function in RV hypertrophy associated with PH. We provide solid evidences that: (**i**) KCNK3 channels are functionally expressed in adult rat RV cardiomyocytes and contribute to action potential repolarization, (**ii**) I_{KCNK3} is reduced during the development of RV hypertrophy in three different experimental models of PH and KCNK3 expression is decreased in one model of chronic RV pressure overload, (**iii**) KCNK3 is expressed in human RV tissues and strongly reduced in RV tissues from PAH patients as compared to non-PAH, (**iv**) chronic specific inhibition of KCNK3 channel induced molecular and electrophysiological alterations which are typically those of RV hypertrophy, and (**v**) chronic specific inhibition of KCNK3 significantly reduces RV cardiac function without significant alteration of LV cardiac function.

We investigated the consequences of the RV hypertrophy by PH and chronic pressure overload in experimental rat models (exposure to MCT, to chronic hypoxia, to Sugen/hypoxia, and to PAB) and its association with on KCNK3 function and other K^+ current determinants. Indeed, eight different mutations have been recently described in human PAH patients[4,5] and we have previously demonstrated a loss of KCNK3 function in the pulmonary vascular cells of patients suffering from idiopathic and heritable PAH, as well as in MCT-rats.[14] We used a selective KCNK3 inhibitor (A293), which is described to inhibit 90% of I_{KCNK3}, 50% of I_{KCNK9} (another K2P channels), and minimally I_{Kv} currents at 1 µmol/L.[8,11] It is noteworthy that KCNK9 mRNA expression which is known to functionally dimerize with KCNK3[18,19] was undetectable in rat RV and LV, and hence cannot be considered as element contributing to RV K^+ current.

The contribution of I_{KCNK3} in action potential repolarization and the membrane resting potential of RV cardiomyocytes, suggests that KCNK3 inhibition or loss of function could facilitate induction of arrhythmias.[20] Indeed, reduced K^+ currents increase the propensity for early after-depolarizations, dispersion of repolarization, and ventricular arrhythmias, thereby significantly increasing the risk of sudden cardiac death in heart failure patients.[21] Here, we demonstrate that action potential repolarization phase was progressively increased during the progression of RV hypertrophy in MCT-rats, and that KCNK3 dysfunction contributes to action potential remodelling. Since the recent demonstration showing that K2P channels, including KCNK3, have rapid and similar voltage sensitivity to many Kv channels,[22] it was not a surprise that KCNK3 contributes to the action potential repolarization in RV cardiomyocytes, property lost in RV hypertrophy associated with pulmonary vascular remodelling or PAB. The functionality of KCNK3 channel can be modulated by local tissue and cellular environmental factors such as several downstream signalling of all Gq-protein-coupled,[23] including endothelin-1 (ET-1) as well as PDGF receptor and tyrosine kinase activity.[24,25] ET-1 is produced in cardiomyocytes[26] and markedly increased in human and MCT failing hearts.[27,28] KCNK3 can also be inhibited by α1A-adrenergic receptor stimulation[8] since their expression are maintained in the LV and RV of the failing human heart.[29] Moreover, KCNK3 is

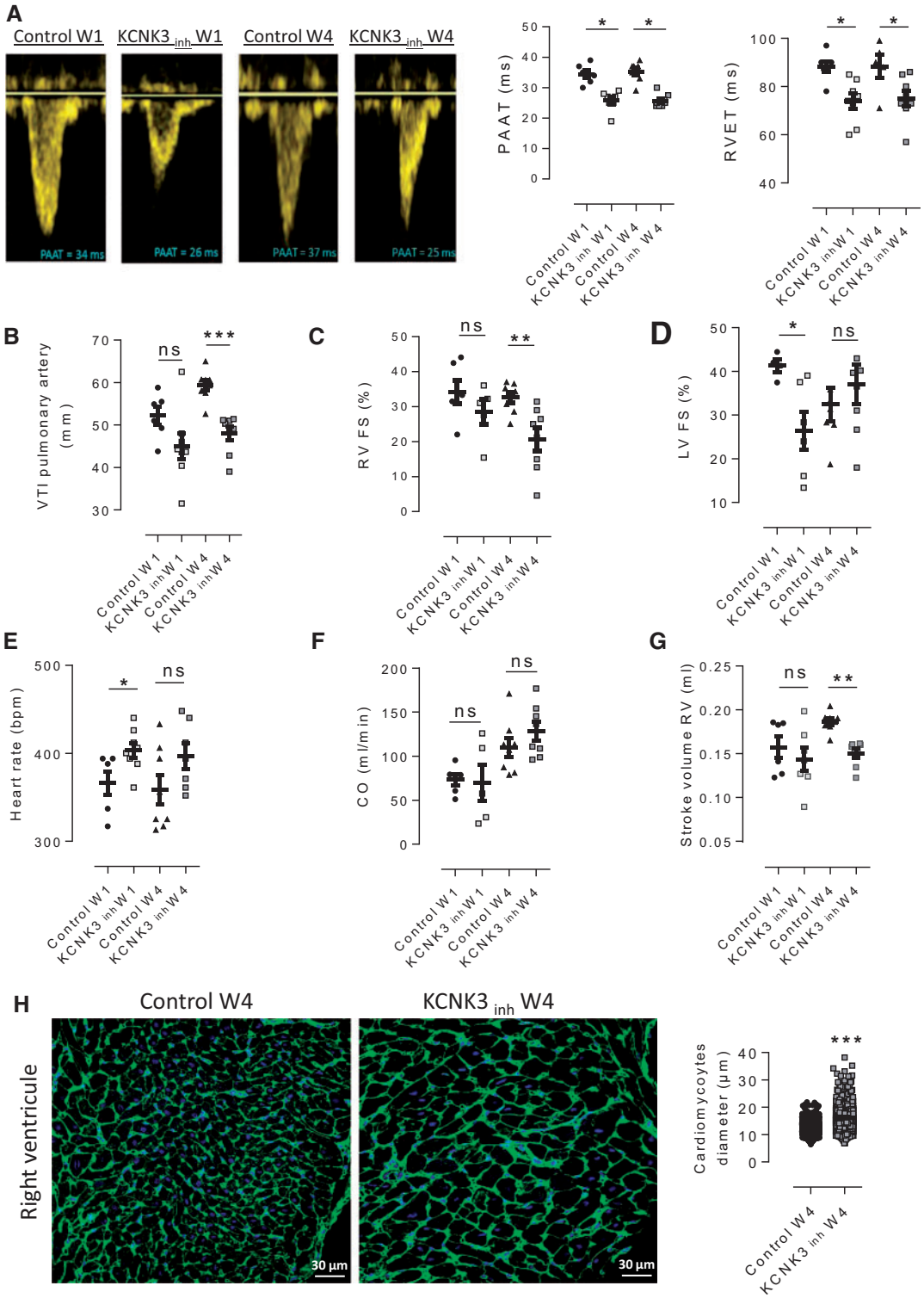

Figure 6 Chronic inhibition of KCNK3 promotes RV dysfunction. (***A***) Representative pulmonary artery flow through the pulmonary valve in control and KCNK3-inhibited (KCNK3 $_{inh}$) rats (W1 and W4, 10 mg/kg/day). Quantification of the pulmonary acceleration time (PAAT) and the right venticular ejection time (RVET). (***B***) Average of velocity time integral (VTI) of pulmonary arteries. (***C***) Right ventricle fractional shortening (RV FS). (***D***) Left ventricle fractional shortening (LV FS). (***E***) Heart rate. (***F***) Cardiac output (CO). (***G***) RV stroke volume in control and KCNK3 $_{inh}$ rats (n = 7–8 different rats). (***H***) Analysis of the level of cardiomyocyte hypertrophy in KCNK3 $_{inh}$ rats. RV sections were stained with FITC-conjugated WGA (50 µg/mL). Right panel: Quantification of cardiomyocytes diameter (10–15 different images per animals from 3–4 different rats, representing 204–234 cardiomyocytes). Compared with control. ns = non-significant, $P < 0.05$*, $P < 0.01$**, $P < 0.001$*** (One-way anova followed by Dunnett's).

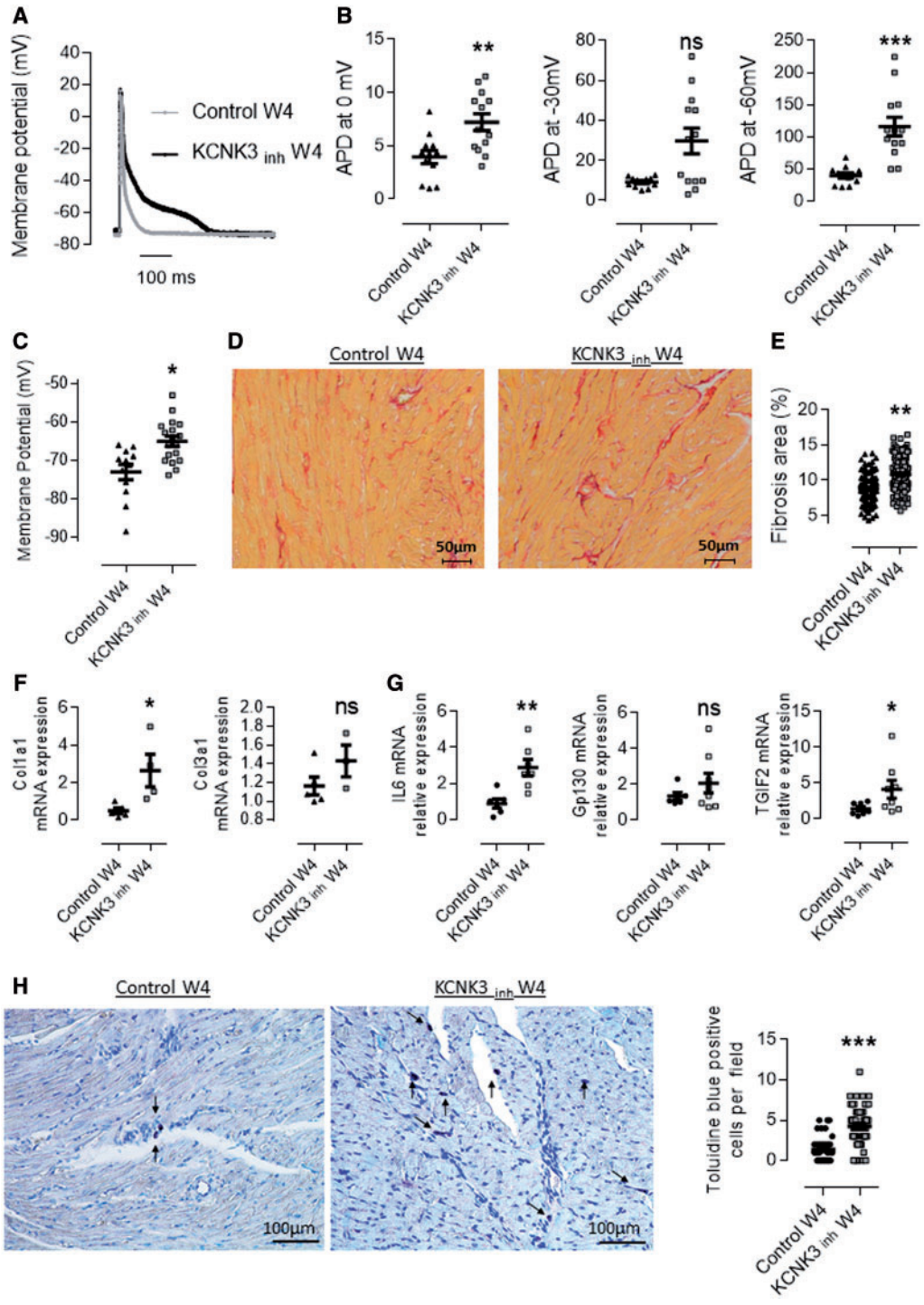

Figure 7 Chronic inhibition of KCNK3 increases RV action potential duration and enhances RV fibrosis. (***A***) Representative membrane potential of RV cardiomyocytes from control rats and KCNK3-inhibited ($KCNK3_{inh}$) rats (W4). Grey trace: control condition. Black trace: KCNK3 inhibitor W4. (***B***) Analysis of RV action potential duration (APD) at 0 mV, APD at –30 mV, and APD at –60mV of membrane repolarization in control rats and $KCNK3_{inh}$ rats (n = 13–18 cells from four different rats). (***C***) Average of resting membrane potential in RV cardiomyocytes isolated from control rats and $KCNK3_{inh}$ rats (W4) (n = 13–18 cells from four different rats). (***D***) Interstitial fibrosis identified with Sirius red staining in RV compartment from control and $KCNK3_{inh}$ rats (at W4). (***E***) Quantification of the percentage of fibrosis in RV tissue from control and $KCNK3_{inh}$ rats (W4) (n = 20 images per rat from 3–4 different rats). (***F***) mRNA expression of Col3a1 and Col1a1 in RV isolated from control rats and $KCNK3_{inh}$ rats (n = 4–5 different rats). (***G***) mRNA expression of IL-6, gp130, and TGIF2 in RV isolated from control rats and $KCNK3_{inh}$ rats (n = 6–7 different rats). (***H***) Section of RV tissue from control and $KCNK3_{inh}$ rats analysed by Toluidine Blue (Toluidine Blue positive mature mast cells are pointed by black arrows). Right panel: quantification of the mature mast cells numbers in RV tissue from control and $KCNK3_{inh}$ rats (n = 10–12 images per animals from 3–4 different rats). Compared with control. ns = non-significant, $P < 0.05$*, $P < 0.01$**, $P < 0.001$*** (Nested anova for patch-clamp experiments. Other experiments were analysed using one-way anova followed by Dunnett's).

sensitive to pH and O_2.[6] The RV compartment of PAH patients and experimental-pulmonary hypertension rats have been described to be less oxygenated[30,31] due to a reduction of angiogenesis, which could in turn contribute to KCNK3 loss of function.

Additional K^+ channels including Kv4.3, Kv4.2, Kir2.1, CaV1.2, CaV3.1, Kv7.1, Kv11.1, Kir3.1 play a key role in action potential repolarization, and we showed a strong reduction of I_{to} in RVH, via Kv4.2, and Kv4.3, which alter the AP repolarization phase observed in PH.[32] An alteration of voltage-gated Ca^{2+} channel (CaV1.2, CaV3.1) expression was described to contribute to action potential remodelling in RV cardiomyocytes from MCT rats.[33] Temple and colleagues also demonstrated a decrease in the expression of KCNK3 in RV from MCT-exposed rats.[34] Here, we presented a severe RV-specific decrease in KCNK3 expression and function in three different rat models of PH and one rat model of chronic RV pressure overload (exposure to MCT, to chronic hypoxia, to Sugen/hypoxia and to PAB), and in human PAH RV tissues, demonstrating that loss of KCNK3 function is a hallmark of RV hypertrophy. QPCR results obtained from frozen RV and LV tissues form PAB demonstrated that the loss of KCNK3 is independent of pulmonary vasculature remodelling.

Some previous reports from mice or rats demonstrated that genetic inhibition of KCNK3 increases ventricular APD and prolongs QTc interval.[8,12,13] Moreover, chronic KCNK3 inhibition leads to an increase in heart rate as previously shown in *Kcnk3* deficient mice[13] and in *Drosophila* homologue KCNK3 mutant stains.[35] We confirmed that KCNK3 is present in human ventricular tissue, and severely reduced in RV from PAH patients, suggesting that the loss of KCNK3 expression could contribute to RV disorders observed in PAH patients. Furthermore, a recent study showed that the KCNK3 knockdown in human iPSC-derived cardiomyocytes leads to significant prolongation of APD, demonstrating the contribution of KCNK3 in action potential repolarization in human cardiomyocytes.[36] RV cardiomyocytes isolated from KCNK3-inhibited rats presented early-after depolarization events, which are implicated as the primary mechanism promoting arrhythmias in acquired and congenital long QT syndromes including, polymorphic ventricular tachycardia and ventricular fibrillation.[37]

Here, we showed that chronic KCNK3 pharmacological inhibition resulted to a significant increase in RV fibrosis and excessive production of IL-6 which could contribute to the RV loss function. Indeed, decreased cardiac performance does not exclusively originate from dysfunctional cardiomyocytes. Increased collagen content of the heart (fibrosis) may affect myocardial systolic and diastolic function.[38] Inflammation undoubtedly plays a dual role in the development of pulmonary vascular remodelling and RV failure.[39] The increase in IL-6 expression in RV tissues from chronic KCNK3 inhibited-rats could partly explain the decrease of RV contractility observed in these animals. Indeed abnormal cytokine expression was shown to impair myocardial contractility via multiple mechanisms.[39] Moreover, *in vivo* administration of IL-6 to rats reduces cardiac contractility in a dose-dependent manner.[40] Furthermore, mast cell density correlates with myocardial fibrosis in congestive heart failure patients.[41] Mast cells have also been described to produce a myriad of cytokines and growth factors such as IL-6.[42–44] PAH patients with higher IL-6 levels are described to have more severe RV dysfunction.[45]

Our results showing that long term KCNK3 inhibition is associated with loss of RV function and our previous work showing pulmonary vascular remodelling in KCNK3-inhibited rats[14] highlight likely cardiopulmonary side effects of pharmacological inhibition of KCNK3 as already suggested by Olschewski *et al.*[46]

4.1 Conclusions

This work strongly suggests for the first time that KCNK3 channel dysfunction is a hallmark of RV hypertrophy. The demonstration that abnormalities in KCNK3 current are temporally, proportionately and specifically associated with RV cardiomyocyte hypertrophy and impairment of RV action potential repolarization in a manner that partially mimics the cardiac phenotype induced by PH is particularly striking. Additionally, our results support the idea that the RV function of PAH patients carrying a *KCNK3* mutation should be more severely affected than KCNK3 mutation non-carriers.

4.2 Limitations

Our results did not specifically exclude a direct effect of KCNK3 inhibition on RV function. The generation of cardiac specific *Kcnk3* deficient animal will constitute a powerful tool to further decipher its association with RV remodelling. Taking advantage of the fact that the KCNK3 channel is non-functional in mouse pulmonary vasculature[47] but functionally expressed in the mouse heart,[13] an alternative strategy may be to study RV histology and detailed cellular/molecular phenotyping in KCNK3 knockout mice.

Supplementary material

Supplementary material is available at *Cardiovascular Research* online.

Acknowledgements

The authors acknowledge from Sanofi-Aventis R&D for A293 compound. The authors thank Dr. J. Sabourin from Inserm UMR S1180, Faculté de Pharmacie, Université Paris Sud, Université Paris-Saclay for critical reading of the manuscript. The authors are grateful to Dr. André Capderou for excellent statistic expertize.

Conflict of interest: M.H. has relationships with drug companies including Actelion, Bayer, GSK, Novartis, and Pfizer. Other authors report no conflicts.

Funding

This work was supported by Laboratoire d'Excellence (LabEx) en Recherche sur le Médicament et l'Innovation Thérapeutique (LERMIT). F.P. receives funding from National Funding Agency for Research (ANR) (Grant ANR-13-JSV1-0011-01) and from Fondation du Grand défi Pierre Lavoie. F.A. is supported by a post-doctoral grant from Aviesan (ITMO IHP). A.H. is supported by a PhD grant from Région Ile de France (CORDDIM). F.A receives funding from the Fondation du Souffle et Fonds de Dotation « Recherche en Santé Respiratoire », from the Fondation Lefoulon-Delalande and from the Fondation Legs Poix. Our research unit is also supported by the patient association HTAPFrance.

References

1. Galiè N, Manes A, Negro L, Palazzini M, Bacchi-Reggiani ML, Branzi A. A meta-analysis of randomized controlled trials in pulmonary arterial hypertension. *Eur Heart J* 2008;**30**:394–403.
2. Humbert M, Lau EMT, Montani D, Jaïs X, Sitbon O, Simonneau G. Advances in therapeutic interventions for patients with pulmonary arterial hypertension. *Circulation* 2014;**130**:2189–2208.
3. Soubrier F, Chung WK, Machado R, Grünig E, Aldred M, Geraci M, Loyd JE, Elliott CG, Trembath RC, Newman JH, Humbert M. Genetics and genomics of pulmonary arterial hypertension. *J Am Coll Cardiol* 2013;**62**:D13–D21.

4. Ma L, Roman-Campos D, Austin ED, Eyries M, Sampson KS, Soubrier F, Germain M, Trégouët D-A, Borczuk A, Rosenzweig EB, Girerd B, Montani D, Humbert M, Loyd JE, Kass RS, Chung WK. A novel channelopathy in pulmonary arterial hypertension. *N Engl J Med* 2013;**369**:351–361.
5. Navas Tejedor P, Tenorio Castaño J, Palomino Doza J, Arias P, Gordo G, López Meseguer M, Román Broto A, Lapunzina P, Escribano Subías P. An homozygous mutation in KCNK3 is associated with an aggressive form of hereditary pulmonary arterial hypertension. *Clin Genet* 2017;**91**:453–457.
6. Lesage F, Lazdunski M. Molecular and functional properties of two-pore-domain potassium channels. *Am J Physiol Renal Physiol* 2000;**279**:F793–F801.
7. Wanstall JC. The pulmonary vasodilator properties of potassium channel opening drugs. *Gen Pharmacol* 1996;**27**:599–605.
8. Putzke C, Wemhöner K, Sachse FB, Rinné S, Schlichthörl G, Li XT, Jaé L, Eckhardt I, Wischmeyer E, Wulf H, Preisig-Müller R, Daut J, Decher N. The acid-sensitive potassium channel TASK-1 in rat cardiac muscle. *Cardiovasc Res* 2007;**75**:59–68.
9. Wiedmann F, Schmidt C, Lugenbiel P, Staudacher I, Rahm A-K, Seyler C, Schweizer PA, Katus HA, Thomas D. Therapeutic targeting of two-pore-domain potassium (K(2P)) channels in the cardiovascular system. *Clin Sci* 2016;**130**:643–650.
10. Enyedi P, Czirják G. Molecular background of leak K+ currents: two-pore domain potassium channels. *Physiol Rev* 2010;**90**:559–605.
11. Schmidt C, Wiedmann F, Voigt N, Zhou X-B, Heijman J, Lang S, Albert V, Kallenberger S, Ruhparwar A, Szabó G, Kallenbach K, Karck M, Borggrefe M, Biliczki P, Ehrlich JR, Baczkó I, Lugenbiel P, Schweizer PA, Donner BC, Katus HA, Dobrev D, Thomas D. Upregulation of K(2P)3.1 K+ current causes action potential shortening in patients with chronic atrial fibrillation. *Circulation* 2015;**132**:82–92.
12. Seyler C, Li J, Schweizer PA, Katus HA, Thomas D. Inhibition of cardiac two-pore-domain K+ (K2P) channels by the antiarrhythmic drug vernakalant–comparison with flecainide. *Eur J Pharmacol* 2014;**724**:51–57.
13. Decher N, Wemhöner K, Rinné S, Netter MF, Zuzarte M, Aller MI, Kaufmann SG, Li XT, Meuth SG, Daut J, Sachse FB, Maier SKG. Knock-out of the potassium channel TASK-1 leads to a prolonged QT interval and a disturbed QRS complex. *Cell Physiol Biochem* 2011;**28**:77–86.
14. Antigny F, Hautefort A, Meloche J, Belacel-Ouari M, Manoury B, Rucker-Martin C, Péchoux C, Potus F, Nadeau V, Tremblay E, Ruffenach G, Bourgeois A, Dorfmüller P, Breuils-Bonnet S, Fadel E, Ranchoux B, Jourdon P, Girerd B, Montani D, Provencher S, Bonnet S, Simonneau G, Humbert M, Perros F. Potassium Channel Subfamily K Member 3 (KCNK3) contributes to the development of pulmonary arterial hypertension. *Circulation* 2016;**133**:1371–1385.
15. Lee JK, Nishiyama A, Kambe F, Seo H, Takeuchi S, Kamiya K, Kodama I, Toyama J. Downregulation of voltage-gated K(+) channels in rat heart with right ventricular hypertrophy. *Am J Physiol* 1999;**277**:H1725–H1731.
16. Schmidt C, Wiedmann F, Zhou X-B, Heijman J, Voigt N, Ratte A, Lang S, Kallenberger SM, Campana C, Weymann AD, Simone R, Szabo G, Ruhparwar A, Kallenbach K, Karck M, Ehrlich JR, Baczkó I, Borggrefe M, Ravens U, Dobrev D, Katus HA, Thomas D. Inverse remodelling of K2P3.1 K+ channel expression and action potential duration in left ventricular dysfunction and atrial fibrillation: implications for patient-specific antiarrhythmic drug therapy. *Eur Heart J* 2017.
17. Mangiafico SS. R Companion: The Handbook for Biological Statistics. An R Companion for the Hadbook of Biological Statistics. 2015. https://rcompanion.org/rcompanion/a_02.html (8 December 2017, date last accessed).
18. Aller MI, Veale EL, Linden A-M, Sandu C, Schwaninger M, Evans LJ, Korpi ER, Mathie A, Wisden W, Brickley SG. Modifying the subunit composition of TASK channels alters the modulation of a leak conductance in cerebellar granule neurons. *J Neurosci* 2005;**25**:11455–11467.
19. Duprat F, Lesage F, Fink M, Reyes R, Heurteaux C, Lazdunski M. TASK, a human background K+ channel to sense external pH variations near physiological pH. *Embo J* 1997;**16**:5464–5471.
20. Ravens U, Cerbai E. Role of potassium currents in cardiac arrhythmias. *Europace* 2008;**10**:1133–1137.
21. Pogwizd SM, Bers DM. Cellular basis of triggered arrhythmias in heart failure. *Trends Cardiovasc Med* 2004;**14**:61–66.
22. Schewe M, Nematian-Ardestani E, Sun H, Musinszki M, Cordeiro S, Bucci G, Groot BL, de Tucker SJ, Rapedius M, Baukrowitz T. A non-canonical voltage-sensing mechanism controls gating in K2P K(+) channels. *Cell* 2016;**164**:937–949.
23. Wilke BU, Lindner M, Greifenberg L, Albus A, Kronimus Y, Bünemann M, Leitner MG, Oliver D. Diacylglycerol mediates regulation of TASK potassium channels by Gq-coupled receptors. *Nat Comms* 2014;**5**:5540.
24. Boucherat O, Chabot S, Antigny F, Perros F, Provencher S, Bonnet S. Potassium channels in pulmonary arterial hypertension. *Eur Respir J* 2015;**46**:1167–1177.
25. Harleton E, Besana A, Chandra P, Danilo P, Rosen TS, Rosen MR, Argenziano M, Robinson RB, Feinmark SJ. TASK-1 current is inhibited by phosphorylation during human and canine chronic atrial fibrillation. *Am J Physiol Heart Circ Physiol* 2015;**308**:H126–H134.
26. Stawski G, Olsen UB, Grande P. Cytotoxic effect of endothelin-1 during 'stimulated' ischaemia in cultured myocytes. *Eur J Pharmacol* 1991;**201**:123–124.
27. Miyauchi T, Yorikane R, Sakai S, Sakurai T, Okada M, Nishikibe M, Yano M, Yamaguchi I, Sugishita Y, Goto K. Contribution of endogenous endothelin-1 to the progression of cardiopulmonary alterations in rats with monocrotaline-induced pulmonary hypertension. *Circ Res* 1993;**73**:887–897.
28. Sakai S, Miyauchi T, Sakurai T, Kasuya Y, Ihara M, Yamaguchi I, Goto K, Sugishita Y. Endogenous endothelin-1 participates in the maintenance of cardiac function in rats with congestive heart failure. Marked increase in endothelin-1 production in the failing heart. *Circulation* 1996;**93**:1214–1222.
29. Jensen BC, Swigart PM, De Marco T, Hoopes C, Simpson PC. {alpha}1-Adrenergic receptor subtypes in nonfailing and failing human myocardium. *Circ Heart Fail* 2009;**2**:654–663.
30. Potus F, Ruffenach G, Dahou A, Thebault C, Breuils-Bonnet S, Tremblay È, Nadeau V, Paradis R, Graydon C, Wong R, Johnson I, Paulin R, Lajoie AC, Perron J, Charbonneau E, Joubert P, Pibarot P, Michelakis ED, Provencher S, Bonnet S. Downregulation of MicroRNA-126 contributes to the failing right ventricle in pulmonary arterial hypertension. *Circulation* 2015;**132**:932–943.
31. Ryan JJ, Archer SL. The right ventricle in pulmonary arterial hypertension: disorders of metabolism, angiogenesis and adrenergic signaling in right ventricular failure. *Circ Res* 2014;**115**:176–188.
32. Rajdev A, Garan H, Biviano A. Arrhythmias in pulmonary arterial hypertension. *Prog Cardiovasc Dis* 2012;**55**:180–186.
33. Benoist D, Stones R, Drinkhill M, Bernus O, White E. Arrhythmogenic substrate in hearts of rats with monocrotaline-induced pulmonary hypertension and right ventricular hypertrophy. *Am J Physiol Heart Circ Physiol* 2011;**300**:H2230–H2237.
34. Temple IP, Logantha SJRJ, Absi M, Zhang Y, Pervolaraki E, Yanni J, Atkinson A, Petkova M, Quigley GM, Castro S, Drinkhill M, Schneider H, Monfredi O, Cartwright E, Zi M, Yamanushi TT, Mahadevan VS, Gurney AM, White E, Zhang H, Hart G, Boyett MR, Dobrzynski H. Atrioventricular node dysfunction and ion channel transcriptome in pulmonary hypertension. *Circ Arrhythm Electrophysiol* 2016;**9**:e003432.
35. Lalevée N, Monier B, Sénatore S, Perrin L, Sémériva M. Control of cardiac rhythm by ORK1, a Drosophila two-pore domain potassium channel. *Curr Biol* 2006;**16**:1502–1508.
36. Chai S, Wan X, Nassal DM, Liu H, Moravec CS, Ramirez-Navarro A, Deschenes I. Contribution of two pore potassium channels to cardiac ventricular action potential revealed using human iPSC-derived cardiomyocytes. *Am J Physiol Heart Circ Physiol* 2017;**312**:H1144–H1153.
37. Weiss JN, Garfinkel A, Karagueuzian HS, Chen P-S, Qu Z. Early afterdepolarizations and cardiac arrhythmias. *Heart Rhythm* 2010;**7**:1891–1899.
38. Bogaard HJ, Abe K, Vonk Noordegraaf A, Voelkel NF. The right ventricle under pressure: cellular and molecular mechanisms of right-heart failure in pulmonary hypertension. *Chest* 2009;**135**:794–804.
39. Role of cardiac inflammation in right ventricular failure.—PubMed—NCBI. https://www.ncbi.nlm.nih.gov/pubmed/28957536 (24 November 2017, date last accessed).
40. Janssen SPM, Gayan-Ramirez G, Van den Bergh A, Herijgers P, Maes K, Verbeken E, Decramer M. Interleukin-6 causes myocardial failure and skeletal muscle atrophy in rats. *Circulation* 2005;**111**:996–1005.
41. Batlle M, Pérez-Villa F, Lázaro A, Garcia-Pras E, Ramirez J, Ortiz J, Orús J, Roqué M, Heras M, Roig E. Correlation between mast cell density and myocardial fibrosis in congestive heart failure patients. *Transplant Proc* 2007;**39**:2347–2349.
42. Conti P, Kempuraj D, Di Gioacchino M, Boucher W, Letourneau R, Kandere K, Barbacane RC, Reale M, Felaco M, Frydas S, Theoharides TC. Interleukin-6 and mast cells. *Allergy Asthma Proc* 2002;**23**:331–335.
43. Krüger-Krasagakes S, Möller A, Kolde G, Lippert U, Weber M, Henz BM. Production of interleukin-6 by human mast cells and basophilic cells. *J Invest Dermatol* 1996;**106**:75–79.
44. Walia DS, Sharma M, Raveendran VV, Zhou J, Sharma R, Stechschulte DJ, Dileepan KN. Human mast cells (HMC-1 5C6) enhance interleukin-6 production by quiescent and lipopolysaccharide-stimulated human coronary artery endothelial cells. *Mediators Inflamm* 2012;**2012**:1.
45. Prins KW, Archer SL, Pritzker M, Rose L, Weir EK, Sharma A, Thenappan T. Interleukin-6 is independently associated with right ventricular function in pulmonary arterial hypertension. *J Heart Lung Transplant* 2017;pii: S1053-2498(17)31985-X.
46. Olschewski A, Chandran N, Olschewski H. Letter by Olschewski *et al.* regarding article, 'Upregulation of K2P3.1 K+ current causes action potential shortening in patients with chronic atrial fibrillation.' *Circulation* 2016;**133**:e439.
47. Manoury B, Lamalle C, Oliveira R, Reid J, Gurney AM. Contractile and electrophysiological properties of pulmonary artery smooth muscle are not altered in TASK-1 knockout mice. *J Physiol (Lond)* 2011;**589**:3231–3246.